JOURNAL OF Applied Polymer SCIENCE

# Dual Action Bactericides: Quaternary Ammonium/*N*-Halamine-Functionalized Cellulose Fiber

**Bojian Hu, Xiaoqin Chen, Yan Zuo, Zuliang Liu, Xiaodong Xing**
College of Chemical Engineering, Nanjing University of Science and Technology, Nanjing 210094, China
Correspondence to: X. Xing (E-mail: xingxiaodong07@njust.edu.cn)

**ABSTRACT:** Bi-functional antibacterial material was prepared by co-grafting *N*-halamine and quaternary ammonium salt monomers from cellulose fiber. The grafted fiber was characterized by Fourier transform infrared spectra, and X-ray photoelectron spectra. The *N*-halamine derived from the precursor 4-[(acryloxy)methyl]-4-ethyl-2-oxazolidinone via chlorination treatment and the oxidative chlorine ($Cl^+$) leaching behavior were investigated. The antibacterial activities of singly (only QAs-functionalized or only $Cl^+$-releasing) and dual (QAs-functionalized and $Cl^+$-releasing) functional cellulose fibers were tested against Gram-negative *Escherichia coli* and Gram-positive *Staphylococcus aureus*. Compared to singly functionalized formulations, the bi-functional cellulose fiber exhibited excellent and rapid bactericidal performance against both *E. coli* and *S. aureus*. © 2013 Wiley Periodicals, Inc. J. Appl. Polym. Sci. **2014**, *131*, 40070.

**KEYWORDS:** N-halamine; quaternary ammonium salt; antibacterial; bi-functional; grafted cellulose fiber

Received 29 July 2013; accepted 16 October 2013
**DOI: 10.1002/app.40070**

## INTRODUCTION

Microbial infections on many commercial applications such as textiles, food packaging and storage, water purification, and medical devices have become a serious public concern.[1–3] Therefore, more research into effective alternative materials with bactericidal properties is needed. There are mainly three strategies to render materials antibacterial: adhesion resistance, contact killing, and biocide agent leaching.[4] However, each of these antibacterial approaches has its own advantages in certain circumstances but disadvantages in other setting.[5] Efforts toward new antibacterial strategies that exert the merits of existing approaches while minimizing the defects have become mainstream trend.[4,6,7]

Quaternary ammonium salts (QAs) are a popular antibacterial component applied to polymers,[8,9] cellulose,[10] films,[11,12] and particles,[13,14] due to their broad-spectrum efficacy, and the ability to kill bacterial with no impact on the QAs structure.[15] Antibacterial activity of short alkyl chained QAs likely results from the positively charged ammonium group favor interaction with negatively charged bacterial cell membrane to disrupt membrane barrier function, break the balance of essential ions, disturb protein activity, and damage bacterial genetic material. Long alkyl chained QAs can use additional antibacterial activity by inserting into the bacterial membrane, resulting in physical disruption.[16] Unfortunately, when the QAs are immobilized, their antibacterial activities may be greatly limited because their diffusion into cell membranes is impeded.[17,18] Thus, integrating QAs functionalities with a second releasable agent might increase the materials' bactericidal performance and benefit from the advantages of combination strategies discussed above. Actually, QAs-modified polymers endowed releasable silver ions ($Ag^+$) exhibited greater antibacterial performance than QAs polymers alone.[19–21]

Over the past few decades, increasingly concern has focused on the development of novel heterocyclic bactericidal *N*-halamine derivatives which have long-term stabilities in contact with aqueous solution as well as in dry storage.[22] Consequently, the focus of this report is creation of *N*-halamine antibacterial coatings for textiles and hard surfaces.[23,24] The 4-[(acryloxy)methyl]-4-ethyl-2-oxazolidinone (AEO), an *N*-chlorohydantoin, acquire great attention because of their potential for economical disinfection of potable water.[25] The bactericidal action of *N*-halamine was ascribed to a chemical reaction involving the transfer of positive halogens from the *N*-halamines to appropriate receptors in the cells. This process can effectively destroy or inhibit the enzymatic or metabolic cell processes, resulting in the expiration of the organisms.[26] The *N*-halamines based therapeutics have the ability to immobilize high concentrations of chlorine to enable rapid bactericidal activities, the capability of recharge upon exposure to aqueous free halogen after the initial halogen is spent, and the release of very low amounts of corrosive free chlorine into water (less than 1 mg $L^{-1}$).[25]

© 2013 Wiley Periodicals, Inc.

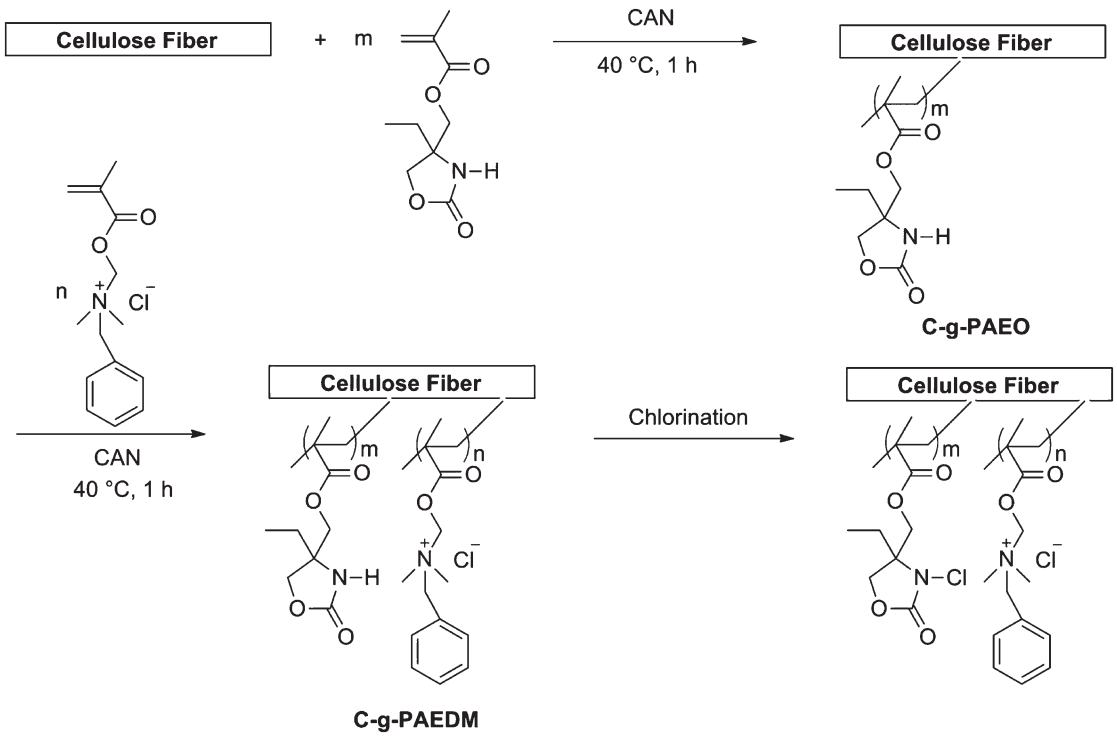


**Scheme 1.** Illustration of the synthesis procedure of antibacterial cellulose fibers.

Cellulose fiber, the first most abundant polysaccharide in the nature, has received much attention. Nature fiber is well-poised for combination therapies due to their versatility, chemical flexibility, biodegradability.[27]

*N*,*N*-Dimethyl-*N*-(methacryloyloxy) ethyl-*N*-benzyl ammonium chloride (DMABn) and their polymer both perform excellent antibacterial propeties.[28] We have previously reported that the sterilization process of DMABn-functionalized cellulose fiber was composed of two steps, in which the adsorption of bacteria on fiber surface driven by electrostatic interaction was a fast process, and cell-lysis was a relatively slow process.[29] In this work, "release-killing" AEO and "contact-killing" DMABn were co-grafting polymerized on cellulose fiber using ceric ammonium nitrate (CAN) as initiator to obtain a bi-functional "attacking antibacterial material" that aiming to thoroughly eliminate bacteria (Scheme 1). We suppose that the composition of quaternary ammoniums with *N*-halamine derivatives into cellulose fiber may result in an increased efficacy compared to singly functionalized cellulose fiber. Herein, the role of QAs and active chlorine was investigated on the bactericidal efficacy against *Escherichia coli* and *Staphylococcus aureus*, which are representative of Gram-negative and Gram-positive bacteria.

## EXPERIMENTAL

### Materials

Cellulose fiber was purchased from Shanghai DaiDi Medical Equipment (China). The monomers 4-[(acryloxy)methyl]-4-ethyl-2-oxazolidinone (AEO) and *N*,*N*-dimethyl-*N*-(methacryloyloxy)-ethyl-*N*-benzyl ammonium chloride (DMABn) were prepared in our laboratories.[29] The initiator CAN was obtained from Adamas Reagent (Basel, Switzerland). Acetone, absolute ethanol, acetic acid, hydrochloric acid, and potassium iodide were purchased from Shanghai Aladdin Chemistry (China). Sodium thiosulfate pentahydrate, sodium hydroxide, potassium dihydrogen phosphate, disodium hydrogen phosphate, sodium chloride, potassium chloride, and sodium hypochlorite solution were purchased from Nanjing Chemical Reagent (China). All reagents were used without any purification.

### Measurements

Fourier transform infrared (FTIR) spectra were recorded on an IR Prestige-21 spectrometer 32 scans at resolution of 2 $cm^{-1}$. X-ray photoelectron spectroscopy (XPS) was performed with a PHI QUANTERA II SXM X-ray photoelectron spectrometer with a monochromatic Al Kα X-ray as the excitation source. Scanning electron microscopy (SEM) images were obtained with a Quanta 200 at an acceleration voltage of 15 kV.

### Preparation of Functional Grafted Cellulose Fiber

The modified cellulose fiber was prepared according to a graft method reported previously.[30,31] The grafted process of the monofunctional cellulose fiber was showed as Scheme 1. Briefly, cellulose fiber (0.1 g) was immersed in 5 mL deionized water. The required amount of relevant monomer AEO (0.533 g, 2.5 mmol) or DMABn (1.274 g, 4.5 mmol) was added and an $N_2$ was purged for 10 min so as to exclude air. After adding the initiator CAN (0.206 g, 0.375 mmol) and in the inert atmosphere of $N_2$, the reaction was performed at 40°C for 1 h. The product filtrated and extracted with acetone in a soxhlet extractor for 12 h to remove the homopolymer and unreacted monomer. After drying under vacuum, the grafted cellulose fiber Cellulose-graft-polyAEO (C-*g*-PAEO) and Cellulose-graft-polyDMABn (C-*g*-PDMABn) were obtained.

The bi-functional co-grafted cellulose fiber was created in a two-step graft process (Scheme 1). The monomer AEO was first

grafted on cellulose fiber to produce C-*g*-PAEO according to the method above, and then this process was repeated with C-*g*-PAEO and another monomer DMABn after the C-*g*-PAEO was extracted with acetone. After polymerization process, the final product Cellulose-cograft-ployAEODMABn (C-*g*-PAEDM) was extracted with acetone and dried.

The grafting ratio (wt %) of grafted cellulose fiber was calculated using the following formula.

$$\text{grafting ratio (wt\%)} = \frac{W_g - W_0}{W_0} \times 100\% \quad (1)$$

where $W_0$ is initial weight of cellulose fiber and $W_g$ is the dry weight of cellulose fiber after grafting with monomer.

### Oxidative Chlorine Release Measurements

To transform the amino groups into *N*-chlorohydantoin, the AEO-functionalized cellulose fiber was immersed in a chlorine bleach solution and stirred at room temperature for 30 min. The chlorinated cellulose fiber was rinsed with water to remove free chlorine and air dried.[25,32] To determine the loading of oxidative chlorine ($Cl^+$) in chlorinated C-*g*-PAEO and C-*g*-PAEDM, a iodimetric titration method was used as reported earlier.[25] Herein, a certain amount of chlorinated fiber sample was dispersed in a mixed solution of 18 mL ethanol and 2 mL 0.1*N* acetic acid for 1 h. Then two different processing methods were used. The first method, adding 0.3 g KI immediately, and the mixture was titrated with 0.01*N* standardized sodium thiosulfate aqueous solution until the yellow color disappeared at the end point. The second method, adding KI after taking out cellulose sample, and the remained solution was titrated with 0.01*N* standardized sodium thiosulfate. The available $Cl^+$ content of the modified cellulose fiber could then be determined from the equation below:

$$\%\,Cl^+ = \frac{N \times V \times 35.45}{W} \times 100\% \quad (2)$$

where $N$ and $V$ are the normality (equiv/L) and volume (L), respectively, of the $Na_2S_2O_3$ consumed in the titration, and $W$ is the weight (g) of the cellulose fiber sample.

### Bactericidal Assays

The kinetics of antibacterial activity of different cellulose fibers toward *E. coli* (gram-negative) and *S. aureus* (gram-positive) were investigated. Briefly, *E. coli* and *S. aureus* were cultured in Luria Bertani broth for 24 h at 37°C. The bacteria were collected by centrifuge, washed with sterile phosphate buffered saline (PBS), and then resuspended in PBS to a concentration of $10^6$–$10^7$ colony-forming units per milliliter (CFU/mL). Measured amounts of chlorinated C-*g*-PAEO, C-*g*-PDMABn, and chlorinated C-*g*-PAEDM were placed in test tube with 3 mL of $10^6$–$10^7$ CFU/mL of *E. coli* (or *S. aureus*) suspension in PBS. After contact times of 5, 20, 30, 40, and 60 min, 0.03 wt % sodium thiosulfate were added to quench any oxidative free chlorine in the solution without affecting the growth of the bacteria.[26] An aliquot of the bacteria was pipetted out and serially diluted, and 100 $\mu$L of each dilution was plated on Luria Bertani agar plates. The same procedure was also applied to the unmodified cellulose fiber to serve as control (blank). Bacterial viability was assessed by counting the number of colonies formed on the agar plate after incubation at 37°C for 24 h.

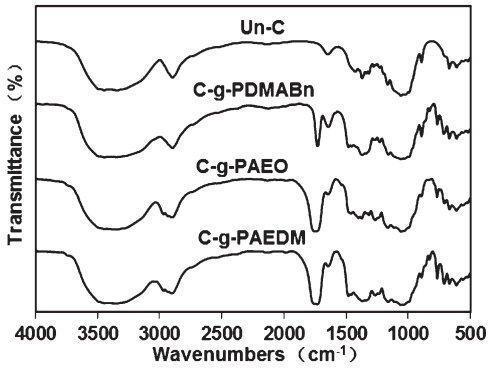


**Figure 1.** FTIR spectra of untreated cellulose (Un-C), cellulose-graft-polyDMABn (C-*g*-PDMABn), cellulose-graft-polyAEO (C-*g*-PAEO), and cellulose-cograft-ployAEODMABn (C-*g*-PAEDM).

Grafted and control cellulose fibers were placed in sterile tube contained *E. coli* for 5 min, respectively. The fiber was gently rinsed in PBS and placed in 2.5% (v/v) glutaraldehyde overnight. The sample was then rinsed three times with PBS, followed by dehydration in a series of ethanol washes. Finally the sample was dried by $CO_2$ critical point, mounted on aluminum stubs, coated with gold/palladium, and imaged in high vacuum mode at 15 kV. The morphology of bacteria in contacted with the cellulose fiber sample was captured.

## RESULTS AND DISCUSSION

### Preparation of Functional Grafted Cellulose Fiber

Three types of grafted cellulose fiber (C-*g*-PAEO, C-*g*-PDMABn, and C-*g*-PAEDM) were prepared via grafting reaction between cellulose fiber and *N*-halamine/QAs monomer (Scheme 1). The two-step graft process resulted in the same content of AEO in C-*g*-PAEO and C-*g*-PAEDM. The grafting ratio of AEO is 45%. Additionally, the content of DMABn in C-*g*-PDMABn and C-*g*-PAEDM was also controlled at the same level. The grafting ratio of DMABn is 56%.

FTIR spectra of C-*g*-PAEO, C-*g*-PDMABn, C-*g*-PAEDM, and the unmodified cellulose fiber were recorded (Figure 1). The spectrum of C-*g*-PDMABn showed strong peak at 1730 $cm^{-1}$ which was assigned to the C═O stretching vibration.[33] The two C═O stretching vibrational modes for any hydantoin compound lead to a broader peak in the 1710–1800 $cm^{-1}$ range which were clearly present for C-*g*-PAEO, and C-*g*-PAEDM. The FTIR spectra of C-*g*-PAEO and C-*g*-PAEDM after chlorination were also investigated (Figure 2). The peak for C═O group of C-*g*-PAEO and C-*g*-PAEDM showed an obvious hypochromatic shift, which was attributed to the inductive effect of chlorine to adjacent carbonyl group. Therefore, the FTIR results verified that AEO and DMABn had been successfully grafted onto cellulose fiber and N—H had been turned into N—Cl in C-*g*-PAEO and C-*g*-PAEDM after chlorination.

Detailed information about the immobilization of AEO and DMABn on cellulose fiber was further provided by XPS

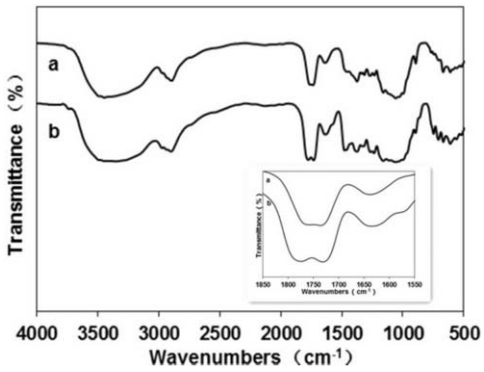


**Figure 2.** FTIR spectra of (a) chlorinated C-*g*-PAEO and (b) chlorinated C-*g*-PAEDM.

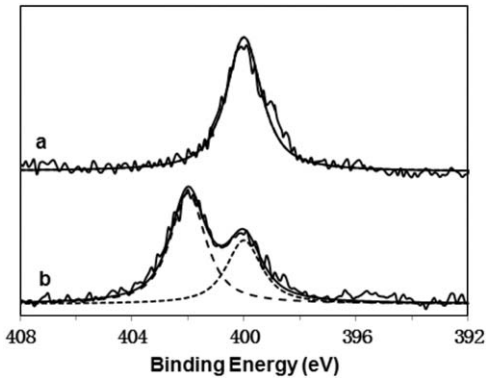


**Figure 4.** High-resolution nitrogen (N 1s) spectra of (a) C-*g*-PAEO and (b) C-*g*-PAEDM.

measurements. XPS spectra of control fiber, C-*g*-PAEO and C-*g*-PAEDM were showed in Figure 3. The unmodified fiber showed the main peaks of C 1s and O 1s at 284 and 533 eV, respectively.[34] As for C-*g*-PAEO, additional new peak of N 1s appeared at about 400 eV, and two new peaks assigned to photoelectrons originating from the Cl 2s and Cl 2p energy level appeared at 272 and 203 eV, respectively, indicating that AEO successfully grafted on cellulose fiber surface.[35] In the spectrum of C-*g*-PAEDM, the characteristic peaks of Cl 2p changed to 199 eV, signifying the presence of the chloride counterion.[36] Further information were supported by the high-resolution nitrogen (N 1s) spectra. As shown in Figure 4(a), the N 1s peak for C-*g*-PAEO appeared at 400 eV, corresponding to the nitrogen in an amide group of AEO.[37] The N 1s peak for C-*g*-PAEDM was fit with two overlapping peaks. The main peak at 402 eV was attributed to nitrogen in a quaternary ammonium. The second peak at 400 eV was assigned to amide functional group [Figure 4(b)].[7] From these results, it is concluded that the AEO and DMABn were successful grafted to cellulose fiber. Additionally, the DMABn grafted layer did not thoroughly cover the AEO layer.

### Oxidative Chlorine Release Measurements

Upon chlorination treatment with sodium hypochlorite bleach, the amino groups in AEO were readily transformed into *N*-halamines for providing the sample with active chlorine. The oxidative chlorine storage and delivery were evaluated by a modified iodometric/thiosulfate titration procedure.[25] Two titration approaches were used, the total loading of oxidative chlorine in the test fiber was determined in the first method, while the amount of active chlorine diffused into surrounding solution was measured in the second method. The different result was apparent from Table I, an evident decrease of active chlorine content was observed after taking out the fiber (i.e., for C-*g*-PAEO, from 5.10 to 0.53%; for C-*g*-PAEDM, from 4.02 to 0.40%). It was concluded that the most of active chlorine was intensively distributed on the grafted fiber, while the concentration of free chlorine keep low in the solution. This result may be attributed to the dissociation equilibrium of *N*-halamines that rendered $Cl^+$ release constant.[26] The leaching behavior had no obvious change with increasing the amount of the sample fiber, which further demonstrated the distribution of active chlorine (Table II). Compared to C-*g*-PAEO, C-*g*-PAEDM leached less active chlorine while the content of AEO in them is the same.

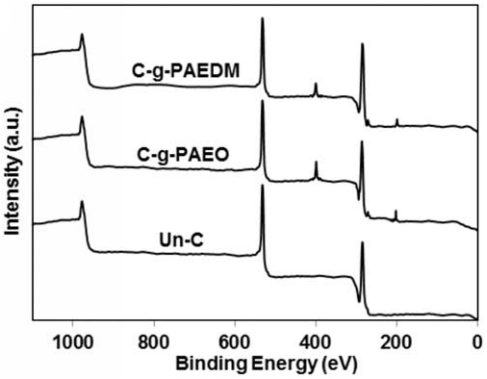


**Figure 3.** X-ray photoelectron (XPS) spectra of untreated cellulose (Un-C), cellulose-graft-polyAEO (C-*g*-PAEO), and cellulose-cograft-ployAEODMABn (C-*g*-PAEDM).

### Bactericidal Efficacy Test

To fully understand the benefit of a combination system, the antibacterial efficacy of the bi-functional cellulose fiber (i.e.,

**Table I.** Comparison of Different Oxidative Chlorine Titration Methods for C-*g*-PAEO and C-*g*-PAEDM

| Cellulose samples | wt % $Cl^{+a}$ | wt % $Cl^{+b}$ |
|---|---|---|
| C-*g*-PAEO | 5.10 | 0.53 |
| C-*g*-PAEDM | 4.02 | 0.40 |

**Table II.** Comparison of Different Oxidative Chlorine Titration Methods for Different amount of C-*g*-PAEDM

| C-*g*-PAEDM (g) | wt % $Cl^{+a}$ | wt % $Cl^{+b}$ |
|---|---|---|
| 0.010 | 4.04 | 0.42 |
| 0.018 | 4.02 | 0.40 |
| 0.032 | 4.06 | 0.45 |

[a] The first titration process that testing cellulose fiber has not been taken out.
[b] The second titration process that testing cellulose fiber has been taken out.

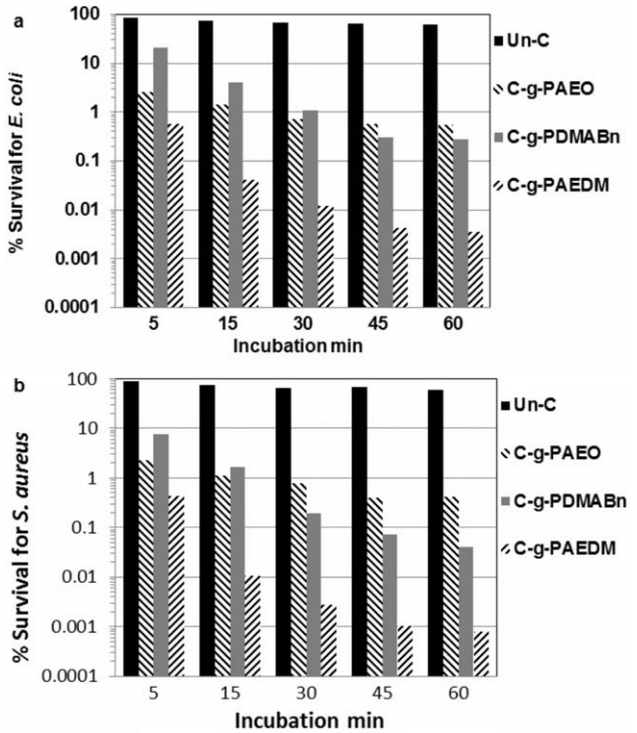


**Figure 5.** Kinetics of antibacterial activity of different cellulose samples toward (a) *E. coli* and (b) *S. aureus*: untreated cellulose (Un-C), cellulose-graft-polyDMABn (C-*g*-PDMABn), cellulose-graft-polyAEO (C-*g*-PAEO), and cellulose-cograft-ployAEODMABn (C-*g*-PAEDM).

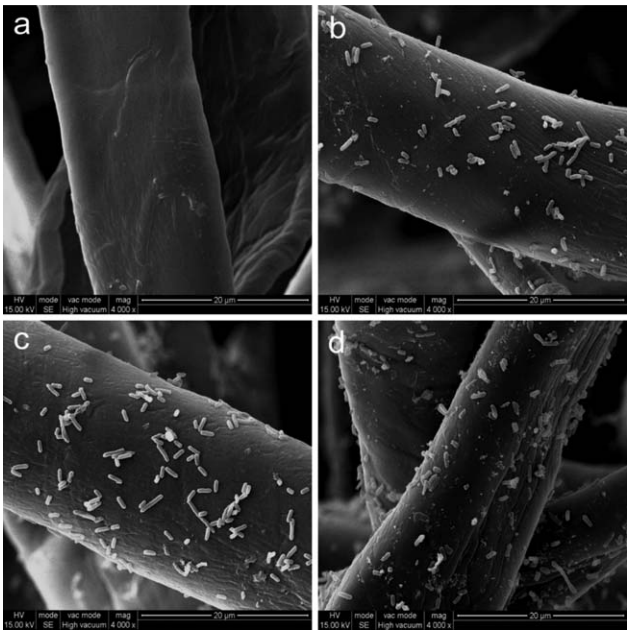


**Figure 6.** SEM image of cellulose samples after contact with *E. coli*: (a) untreated cellulose (control), (b) C-*g*-PAEO, (c) C-*g*-PDMABn, and (d) C-*g*-PAEDM.

C-*g*-PAEDM, contained 4.02% $Cl^+$) against gram-negative bacteria *E. coli* and gram-positive bacteria *S. aureus* was tested compared to the mono-functional formulations alone (i.e., C-*g*-PDMABn or C-*g*-PAEO, contained 5.10% $Cl^+$). The antibacterial assay of the unmodified cellulose fiber was performed by the same method.

The C-*g*-PAEO (contained 5.10% $Cl^+$) showed fast suppression (fast reduction in number of colony-forming units with time) against both *E. coli* and *S. aureus* (Figure 5). However, the suppression only led to about 2 log unit reduction after 60 min contact. This result was consistent with the above researched result that the loaded active chlorine maintained low concentration. Additionally, the antibacterial activity of the C-*g*-PDMABn against *S. aureus* was greater than *E. coli* (Figure 5). Liang et al. also reported greater sensitivity of *S. aureus* to QAs-based antibacterial compared to *E. coli*.[25] This result could be attributed to the compositions of the bacterial cells. It is well known that the bactericidal abilities of QAs derive from the disruption of the cell membrane, followed by leakage of essential cell components, leading to cell death.[38] Gram-negative bacteria such as *E. coli* have more complex cell walls than Gram-positive such as *S. aureus* which resist the penetration by QAs.

The advantages of combining antibacterial system have previously been demonstrated with QAs-functionalized surfaces that release silver ion.[2,6,19] The QAs-functionalized cellulose fiber described herein was allowed to provide active chlorine, a rapid and potent antibacterial.[23] It is interesting to note that, even though the tested QAs-functionalized $Cl^+$-releasing cellulose fiber C-*g*-PAEDM (contained 4.02% $Cl^+$) leached a lower amount of active chlorine, the bi-functional cellulose fiber showed a much more efficient bacterial suppression than $Cl^+$-releasing alone C-*g*-PAEO (contained 5.10% $Cl^+$) and QAs-functionalized alone C-*g*-PDMABn (Figure 5). These observations could be understood in view of the fact that bacteria could be quickly attached to cellulose fiber surface. It has been demonstrated in previous report that the bactericidal mechanism of *N*-halamine polymer does not involve dissociation of the N—Cl bond in aqueous solution to form "free chlorine" (which then acts as the biocidal portion)[18] but the adsorbed bacteria is directly killed. Furthermore, the interaction between bacteria and active chlorine perhaps became more convenient because the permeability of cell membrane is altered by QAs. Thus, integrating quaternary ammonium salt and *N*-halamine derivatives into combination system can achieve both fast and potent antibacterial capacity.

To further investigate the advantage of treatment with QAs-functionalized and $Cl^+$-releasing cellulose fiber, SEM was also performed to observe the morphology of *E. coli* cell adsorbed on cellulose fiber samples (i.e., untreated cellulose, C-*g*-PAEO, C-*g*-PDMABn, and C-*g*-PAEDM) for 5 min [Figure 6(a–d)]. Scarcely any bacteria were found on control fiber surface, which indicated that the cellulose fiber itself has no antibacterial ability. However, many bacteria adhering to fiber were observed on C-*g*-PAEO, C-*g*-PDMABn, and C-*g*-PAEDM surface. Additionally, more bacteria were found on QAs-functionalized cellulose fibers (i.e., C-*g*-PDMABn or C-*g*-PAEDM) assigned to the adsorption capacity of QAs.[16]

Interestingly, beside the fragment of *E. coli* cell, some natural bacteria were also found on C-*g*-PAEO surface. As is known, *N*-halamine had no electrostatic adsorption capacity for bacteria. It was assumed that bacteria around fiber surface were sterilized by $Cl^+$ and then the dead bacteria further adsorbed live bacteria, which could be analogous to the formation process of biofilm.[39] Most of the observed bacteria are intact on C-*g*-PDMABn, but many fragments of bacteria and dead bacteria were observed on C-*g*-PAEDM. These results were consistent with kinetics of antibacterial activity, and demonstrated that QAs-functionalized cellulose fiber quickly adsorbed bacteria without immediately sterilizing them.[29] Conversely, $Cl^+$-releasing cellulose fiber possessed rapid inhibit function but weak adsorption capacity. The bi-functional cellulose fiber used the advantages of two antibacterial mechanisms while minimizing the drawback to exhibit a novel antibacterial action process and perform rapid and highly potent antibacterial efficacy.

## CONCLUSIONS

In summary, three kinds of antibacterial cellulose fibers were prepared by grafting different monomers and their combination. The functionalization of cellulose fiber with both QAs groups and $Cl^+$ donors rendered the material with more efficient antibacterial activity against *E. coli* and *S. aureus* than monofunctional QAs-functionalized or $Cl^+$-releasing cellulose fiber alone. Additionally, the oxidative chlorine was intensely distributed on the surface of cellulose fiber. Because QAs adsorbed microbes to the high concentration area of active chlorine, the dual action antibacterial fiber achieved excellent antibacterial property. The cografted cellulose fiber greatly manifested the superiority of multiple antibacterial mechanisms of action. We believe that QAs and *N*-halamine combined system have potential applications in a wide variety of general field, especially for water sterilization.

## ACKNOWLEDGMENTS

The authors thank the Natural Science Foundation of China (No. 81130078) and NUST Research Funding (No. 2011YBXM54) for financial support.

## REFERENCES

1. Hetrick, E. M.; Schoenfisch, M. H. *Chem. Soc. Rev.* **2006**, *35*, 780.
2. Li, Z.; Lee, D.; Sheng, X.; Cohen, R. E.; Rubner, M. F. *Langmuir* **2006**, *22*, 9820.
3. Aumsuwan, N.; McConnell, M. S.; Urban, M. W. *Biomacromolecules* **2009**, *10*, 623.
4. Ho, C. H.; Tobis, J.; Sprich, C.; Thomann, R. *Adv. Mater.* **2004**, *16*, 957.
5. Lichter, J. A.; Van Vliet, K. J.; Rubner, M. F. *Macromolecules* **2009**, *42*, 8573.
6. Sambhy, V.; MacBride, M. M.; Peterson, B. R.; Sen, A. *J. Am. Chem. Soc.* **2006**, *128*, 9798.
7. Carpenter, A. W.; Worley, B. V.; Slomberg, D. L.; Schoenfisch, M. H. *Biomacromolecules* **2012**, *13*, 3334.
8. Jiang, S.; Wang, L.; Yu, H.; Chen, Y. *React. Funct. Polym.* **2005**, *62*, 209.
9. Yao, C.; Li, X.; Neoh, K. G.; Shi, Z.; Kang, E. T. *J. Membr. Sci.* **2008**, *320*, 259.
10. El-Khouly, A. S.; Kenawy, E.; Safaan, A. A.; Takahashi, Y. *Carbohydr. Polym.* **2011**, *83*, 346.
11. Huang, J.; Koepsel, R. R.; Murata, H.; Wu, W.; Lee, S. B.; Kowalewski, T.; Russell, A. J.; Matyjaszweski, K. *Langmuir* **2008**, *24*, 6785.
12. Dizman, B.; Elasri, M. O.; Mathias, L. J. *J. Polym. Sci. Part A: Polym. Chem.* **2006**, *44*, 5965.
13. Song, J.; Kong, H.; Jang, J. *Colloids Surf. B* **2011**, *82*, 651.
14. Kreutzwiesner, E.; Noormofidi, N.; Wiesbrock, F.; Kern, W.; Rametsteiner, K.; Stelzer, F.; Slugovc, C. *J. Polym. Sci. Part A: Polym. Chem.* **2010**, *48*, 4504.
15. Dong, H.; Huang, J.; Koepsel, R. R.; Ye, P.; Russell, A. J.; Matyjaszewski, K. *Biomacromolecules* **2011**, *12*, 1305.
16. Patel, S. A.; Patel, M. V.; Ray, A.; Patel, R. M. *J. Polym. Sci. Part A: Polym. Chem.* **2003**, *41*, 2335.
17. Singh, P.; Srivastava, A.; Kumar, R. *J. Polym. Sci. Part A: Polym. Chem.* **2012**, *50*, 1503.
18. Muller, R.; Eidt, A.; Hiller, K.-A.; Katzur, V.; Subat, M.; Schweikl, H.; Imazato, S.; Ruhl, S.; Schmalz, G. *Biomaterials* **2009**, *28*, 4921.
19. Song, J.; Kang, H.; Lee, C.; Hwang, S. H.; Jang, J. *ACS Appl. Mater. Interfaces* **2012**, *4*, 460.
20. Kalaycı, Ö. A.; Cömert, F. B.; Hazer, B.; Atalay, T.; Cavicchi, K.; Cakmak, M. *Polym. Bull.* **2010**, *65*, 215.
21. Hazer, D. B.; Mut, M.; Dinçer, N.; Sarıbaş, Z.; Hazer, B.; Özgen, T. *Childs Nervous System* **2012**, *28*, 839.
22. Sun, Y.; Sun, G. *Macromolecules* **2002**, *35*, 8909.
23. Lin, J.; Winkelmann, C.; Worley, S. D.; Broughton, R. M.; Williams, J. F. *J. Appl. Polym. Sci.* **2001**, *81*, 943.
24. Braun, M.; Sun, Y. Y. *J. Polym. Sci. Part A: Polym. Chem.* **2004**, *42*, 3818.
25. Liang, J.; Chen, Y.; Barnes, K.; Wu, R.; Worley, S. D.; Huang, T.-S. *Biomaterials* **2006**, *27*, 2495.
26. Cao, Z.; Sun, Y. *J. Biomed. Mater. Res. Part A* **2008**, *85*, 99.
27. Habibi, Y.; Lucia, L. A.; Rojas, O. *J. Chem. Rev.* **2010**, *110*, 3479.
28. Lu, G. Q.; Wu, D. C.; Fu, R. W. *React. Funct. Polym.* **2007**, *67*, 355.
29. Lu, D. N.; Zhou, X. R.; Xing, X. D.; Wang, X. G.; Liu, Z. *Acta Polym. Sin.* **2004**, *1*, 107.
30. Chen, Z. B.; Sun, Y. Y. *Ind. Eng. Chem. Res.* **2006**, *45*, 2634.
31. Zuo, H. J.; Luo, Z. W.; Wu, D. C.; Fu, R. W. *Acta Scientiarum Naturalium Universitatis Sunyatseni* **2010**, *5*, 61.
32. Liu, S.; Sun, Gang. *Ind. Eng. Chem. Res.* **2009**, *48*, 613.
33. Sun, Y.; Sun, G. *J. Appl. Polym. Sci.* **2001**, *80*, 2460.

34. Xu, Z.; Li, C.; Kang, X.; Yang, D.; Yang, P.; Hou, Z.; Lin, J. *J. Phys. Chem. C* **2010**, *114*, 16343.

35. Claes, M.; Voccia, S.; Detrembleur, C.; Jerome, C.; Gilbert, B.; Leclere, P.; Geskin, V. M.; Gouttebaron, R.; Hecq, M. *Macromolecules* **2003**, *36*, 5926.

36. O'Hare, L.-A.; O'Neill, L.; Goodwin, A. *J. Surf. Interface Anal.* **2006**, *38*, 1519.

37. Xuan, S.; Wang, Y. J.; Leung, K. C.; Shu, K. *J. Phys. Chem. C* **2008**, *112*, 18804.

38. Gottenbos, B.; van der Mei, H. C.; Klatter, F.; Nieuwenhuis, P.; Busscher, H. J. *Biomaterials* **2002**, *23*, 1417.

39. Hoffman, L. R.; Lucas R.; D'Argenio, D. A.; MacCoss, M. J.; Zhang, Z.; Jones, R. A.; Miller, S. I. *Nature* **2005**, *436*, 1171.